AWARD NUMBER: W81XWH-18-1-0613

TITLE: Dkk1 Antagonism for Stromal Vascular Fraction (SVF) Mediated Bone Repair

PRINCIPAL INVESTIGATOR: Aaron W. James, MD, PhD

CONTRACTING ORGANIZATION: Johns Hopkins University, Baltimore, MD

REPORT DATE: January 2024

TYPE OF REPORT: FINAL

PREPARED FOR: U.S. Army Medical Research and Development Command
Fort Detrick, Maryland 21702-5012

REPORT DOCUMENTATION PAGE

Form Approved
OMB No. 0704-0188

1. REPORT DATE	2. REPORT TYPE	3. DATES COVERED
January 2024	Final	30Sep2018-29Sep2023

4. TITLE AND SUBTITLE

Dkk1 Antagonism for Stromal Vascular Fraction (SVF) Mediated Bone Repair

5a. CONTRACT NUMBER
W81XWH-18-1-0613

5b. GRANT NUMBER

5c. PROGRAM ELEMENT NUMBER

6. AUTHOR(S)
Aaron W. James

E-Mail: awjames@jhmi.edu

5d. PROJECT NUMBER

5e. TASK NUMBER

5f. WORK UNIT NUMBER

7. PERFORMING ORGANIZATION NAME(S) AND ADDRESS(ES)

Johns Hopkins University
3400 N Charles St.
Baltimore, MD 21218

8. PERFORMING ORGANIZATION REPORT NUMBER

9. SPONSORING / MONITORING AGENCY NAME(S) AND ADDRESS(ES)

U.S. Army Medical Research and Development Command
Fort Detrick, Maryland 21702-5012

10. SPONSOR/MONITOR'S ACRONYM(S)

11. SPONSOR/MONITOR'S REPORT NUMBER(S)

12. DISTRIBUTION / AVAILABILITY STATEMENT

Approved for Public Release; Distribution Unlimited

13. SUPPLEMENTARY NOTES

14. ABSTRACT

Non-healing bone defects remain a significant problem for combat casualties and military veterans. The gold standard for skeletal regeneration is autograft bone, which is limited in supply, and possesses harvest-related complications. As an alternative, mesenchymal stem cells (MSC) have been employed to accelerate bone regeneration. Yet, current MSC sources have significant drawbacks, including: *(1)* scarce availability, *(2)* need for culture, and *(3)* cell heterogeneity with decreased bone-forming efficacy.

15. SUBJECT TERMS
Bone repair, bone regeneration, bone tissue engineering

16. SECURITY CLASSIFICATION OF:			17. LIMITATION OF ABSTRACT	18. NUMBER OF PAGES	19a. NAME OF RESPONSIBLE PERSON
a. REPORT	b. ABSTRACT	c. THIS PAGE			USAMRDC
Unclassified	Unclassified	Unclassified	Unclassified	19	19b. TELEPHONE NUMBER *(include area code)*

TABLE OF CONTENTS

1. INTRODUCTION

Non-healing bone defects remain a significant problem for combat casualties and military veterans. The gold standard for skeletal regeneration is autograft bone, which is limited in supply, and possesses harvest-related complications. As an alternative, mesenchymal stem cells (MSC) have been employed to accelerate bone regeneration. Yet, current MSC sources have significant drawbacks, including: *(1)* scarce availability, *(2)* need for culture, and *(3)* cell heterogeneity with decreased bone-forming efficacy.

On the backdrop of these significant limitations, our research group has identified a novel, purified and uncultured stem cell source for improved bone tissue regeneration, known as *Perivascular Stem Cells (PSC)*. PSC are prospectively purified ancestors of culture-derived MSC and are identified by their presence around blood vessels. PSC are isolated from adipose tissue by multicolor fluorescence activated cell sorting (FACS). Since the first description of PSC by our research group, we have demonstrated in multiple animal models that PSC induce significantly greater bone regeneration as compared to unpurified stromal cells derived from the same patient's adipose sample (termed stromal vascular fraction or SVF).

Despite the clear cut biologic advantages of PSC for bone regeneration, the level of complexity for cell isolation is high, leading to regulatory challenges in clinical translation. In contrast, a much simpler and more deployable solution from a regulatory standpoint would be to identify those cell signaling components responsible for the poor-bone forming efficacy of SVF or their culture-equivalent (ASC). This advance will allow one to bypass the need for cell purification. Toward this end, whole transcriptome sequencing (RNA Seq) was performed on SVF and PSC from the same patient samples. We screened our transcriptome analysis for extracellular, anti-osteogenic molecules enriched in SVF, and identified the Wnt signaling antagonist DKK1 (Dickkopf-1) as a targetable factor. In pilot studies, use of neutralizing DKK1 antibodies (anti-DKK1) significantly rescued the osteogenic differentiation of adipose-derived MSC in culture.

2. KEYWORDS

Mesenchymal stem cell, adipose stem cell, adipose-derived stem/stromal cell, osteoprogenitor cell, bone healing, bone regeneration spine fusion, Wnt signaling, DKK1, Anti-DKK1

3. ACCOMPLISHMENTS

What were the major goals of the project?

The project contains three aims:

Aim 1: Determine how DKK1 antagonism impacts human ASC lineage commitment *in vitro*.
Aim 2: Validate the combination of anti-DKK1 and SVF in femoral bone defect regeneration.
Aim 3: Challenge anti-DKK1 + SVF therapy in osteoporotic lumbar spinal fusion.

What was accomplished under these goals?

- DKK1 antagonism and it's in vitro effects

Gene expression of the Wnt signaling antagonists *DKK1* (Dickkopf 1) and *SOST* (Sclerostin) were first assessed across time during the osteogenic differentiation of human ASC by qRT-PCR (**Fig. 1A,B**). Results showed that the levels of *DKK1* transcripts peaked early in osteogenic differentiation (90% increase at d 3, $^{**}P<0.01$) and returned to slightly below baseline at d 7 and 10 of differentiation (50% reduction from baseline expression at d 10). The levels of *SOST* transcripts followed a similar trend with a slight increase at d 3 of osteogenic differentiation (31% increase, which did not reach statistical significance), followed by a reduction by 10 d (38% reduction from baseline at d 10). The cellular effects of neutralizing antibodies to either DKK1 or SOST were next assessed. In each case, control cells were treated with an IgG isotype control at the same concentration. When neutralizing anti-DKK1 antibody was used to treat ASCs during culture, a slightly higher proliferative rate was observed, assessed by MTS assays (2% increase at 72 h, **Fig. 1C**). In addition, anti-DKK1 treatment promoted osteogenic differentiation dose-dependently, starting from the 1μg/mL (**Fig. 1D,E**). This was detected by alizarin red staining (**Fig. 1D**) for bone nodule deposition and quantification (**Fig. 1E**, 13-40% increase from 0.5-4 μg/mL). In contrast, across a wide range of concentrations anti-SOST did not increase ASC osteogenic differentiation at any dosage (**Fig. 1F,G**).

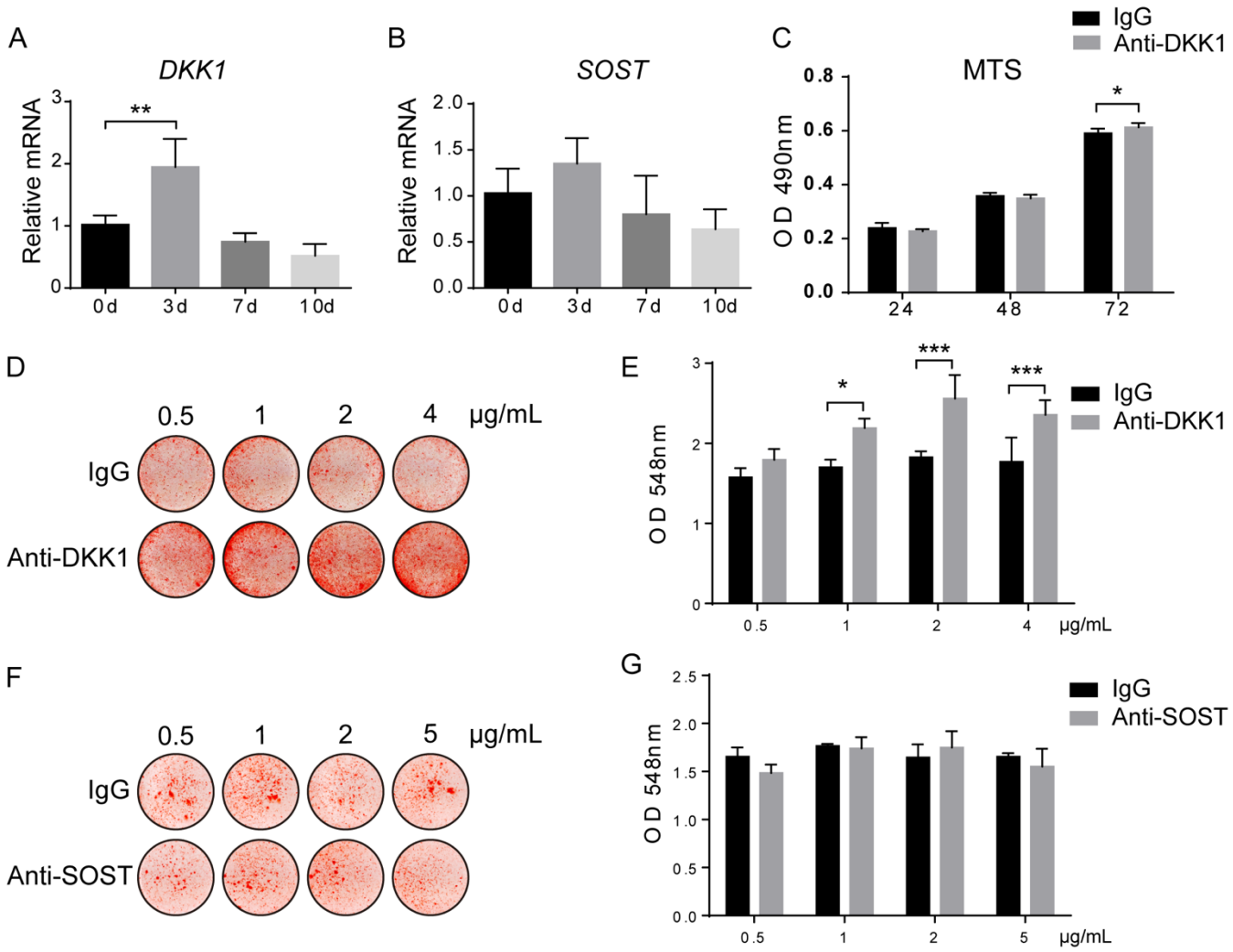

Figure 1. Anti-DKK1 but not anti-SOST enhances the osteogenic differentiation of human adipose-derived stem/stromal cells (ASC). (A,B) Gene expression of Dickkopf 1 (*DKK1*) and Sclerostin (*SOST*) across time during the osteogenic differentiation of human ASC (0-10 d of differentiation). Each group of different time points was compared with that of 0 d. **(C)** Effects of anti-DKK1 on ASC proliferation, assessed by MTS assay at 24-72 h (1 µg/mL). **(D,E)** Effects of anti-DKK1 on ASC osteogenic differentiation, assessed by alizarin red staining and quantification after 7 d differentiation (0.5-4 µg/mL). Whole well images shown. **(F,G)** Effects of anti-SOST on ASC osteogenic differentiation, assessed by alizarin red staining and quantification after 7 d differentiation (0.5-5 µg/mL). All experiments performed with an appropriate isotype IgG control. Experiments performed in at least experimental and biological triplicate. Error bars represent one standard deviation. **P*<0.05; ***P*<0.01; ****P*<0.001.

Overall, we observed an increase in ASC osteogenesis with anti-DKK1 but not anti-SOST treatment. To confirm and expand on this observation, we next assessed changes in osteogenic gene expression by qRT-PCR with anti-DKK1 or isotype control treatment (**Fig. 2A-C**). Results showed a significant increase in osteogenic gene expression among anti-DKK1 treated samples in comparison to IgG isotype control. This included increased expression of the master osteogenic transcription factor *RUNX2* (runt related transcription factor 2, 1.8-fold increase, **Fig. 2A**) and the enzyme *ALP* (alkaline phosphatase, 82% increase, **Fig. 2B**). A trend toward an increase in the bone matrix encoding gene *COL1A1* (Collagen Type I Alpha 1) was also observed (26% increase, **Fig. 2C**).

Next, we assessed gene expression of markers indicative of overall canonical Wnt signaling activity, including *AXIN2* (Axis Inhibition Protein 2) and *CCND1* (Cyclin D1) (**Fig. 2D,E**). Confirming bioactivity of anti-DKK1, both gene transcripts were more highly expressed among anti-DKK1 treated cells in comparison to isotype control (2.4-fold and 65% increase in *AXIN2* and *CCND1* transcripts, respectively). Furthermore, western blot for total β-catenin expression confirmed activation of canonical Wnt signaling pathway after anti-DKK1 treatment (**Fig. 2F**).

Neutralization of a Wnt antagonist such as DKK1 may lead to compensatory changes, such as increased transcription of the same or other Wnt antagonists. Such compensatory changes have been reported with anti-DKK1 treatment in rodent models. To investigate, we examined gene expression of both *DKK1* and *SOST* after anti-DKK1 treatment. Results indicated that anti-DKK1 induced no change in *DKK1* expression (**Fig. 2G**). In contrast, anti-DKK1 led to a significant increase in *SOST* transcript abundance (**Fig. 2H**, 72% increase in *SOST* transcripts).

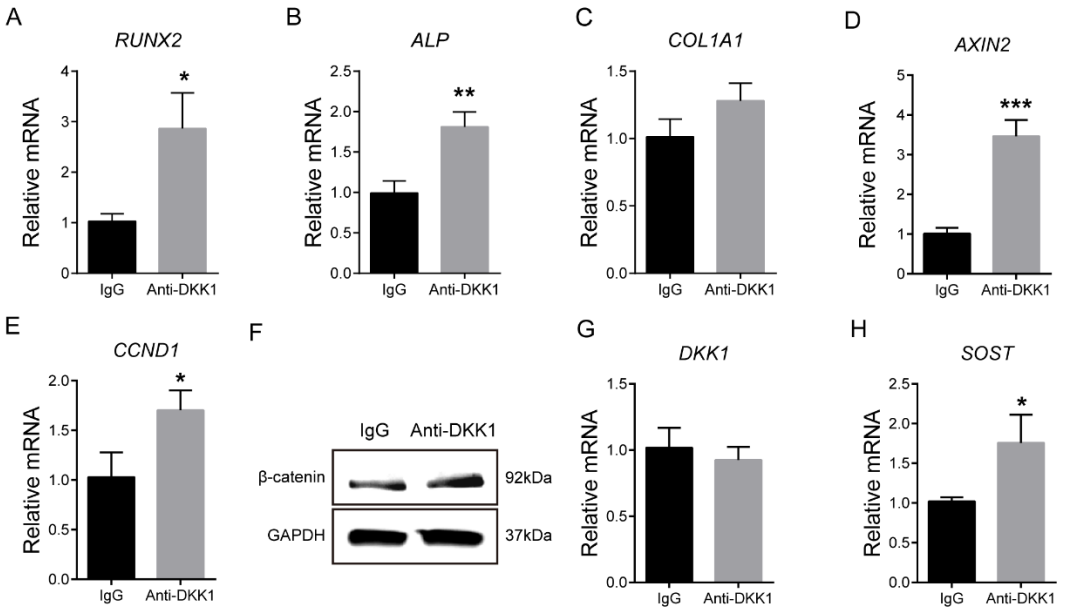

Figure 2. Anti-DKK1 induces changes in osteogenic and Wnt signaling related genes in human ASC. (A-C) Gene expression during osteogenic with anti-DKK1 treatment for 3 d, including **(A)** *RUNX2* (Runt related transcription factor 2), **(B)** *ALP* (Alkaline phosphatase) and **(C)** *COL1A1* (Collagen Type I Alpha 1). **(D,E)** Wnt signaling gene expression with anti-DKK1 (1 μg/mL) treatment for 3 d, including **(D)** *AXIN2* (Axis Inhibition Protein 2) and **(E)** *CCND1* (Cyclin D1). **(F)** Total β-catenin expression with anti-DKK1 treatment for 1 d by western blot. **(G, H)** Gene expression of Wnt signaling antagonists with anti-DKK1 (1 μg/mL) treatment for 3 d, including **(G)** *DKK1* (Dickkopf-1), and **(H)** *SOST* (Sclerostin). All experiments performed with an appropriate isotype IgG control. Experiments performed in at least experimental and biological triplicate. Error bars represent one standard deviation. **P*<0.05; ***P*<0.01; ****P*<0.001.

In order to confirm the anti-DKK1 neutralizing function further, we employed recombinant DKK1 to impair osteogenic differentiation in ASC. Results demonstrated that DKK1 treatment decreased mineralization at a concentration of 50 ng/mL, but not at lower concentrations (**Fig. 3A)**. Next, anti-DKK1 was supplemented with DKK1 during osteogenic differentiation conditions. Here, anti-DKK1 rescued the impairment of osteogenesis induced by recombinant DKK1 (**Fig. 3B**). After baseline effects of anti-DKK1 treatment were determined, the effects of timing of DKK1 neutralization on ASC osteogenesis were assessed (**Fig. 3C-E)**. Anti-DKK1 supplemented at early timepoints of differentiation (treatment beginning at either d 0 or d 3) led to an increase in ASC osteogenic differentiation (**Fig. 3C,D**). This was quantified to determine an 9% and 20% increase in mineralization if anti-DKK1 treatment was initiated at d 0 and d 3, respectively. In contrast, initiating anti-DKK1 treatment at the later timepoint of d 5 of differentiation had no significant effect on mineralization (**Fig. 3E**). This observation was concordant with the peak of expression levels of *DKK1* during early osteogenic differentiation (see again **Fig. 1A**).

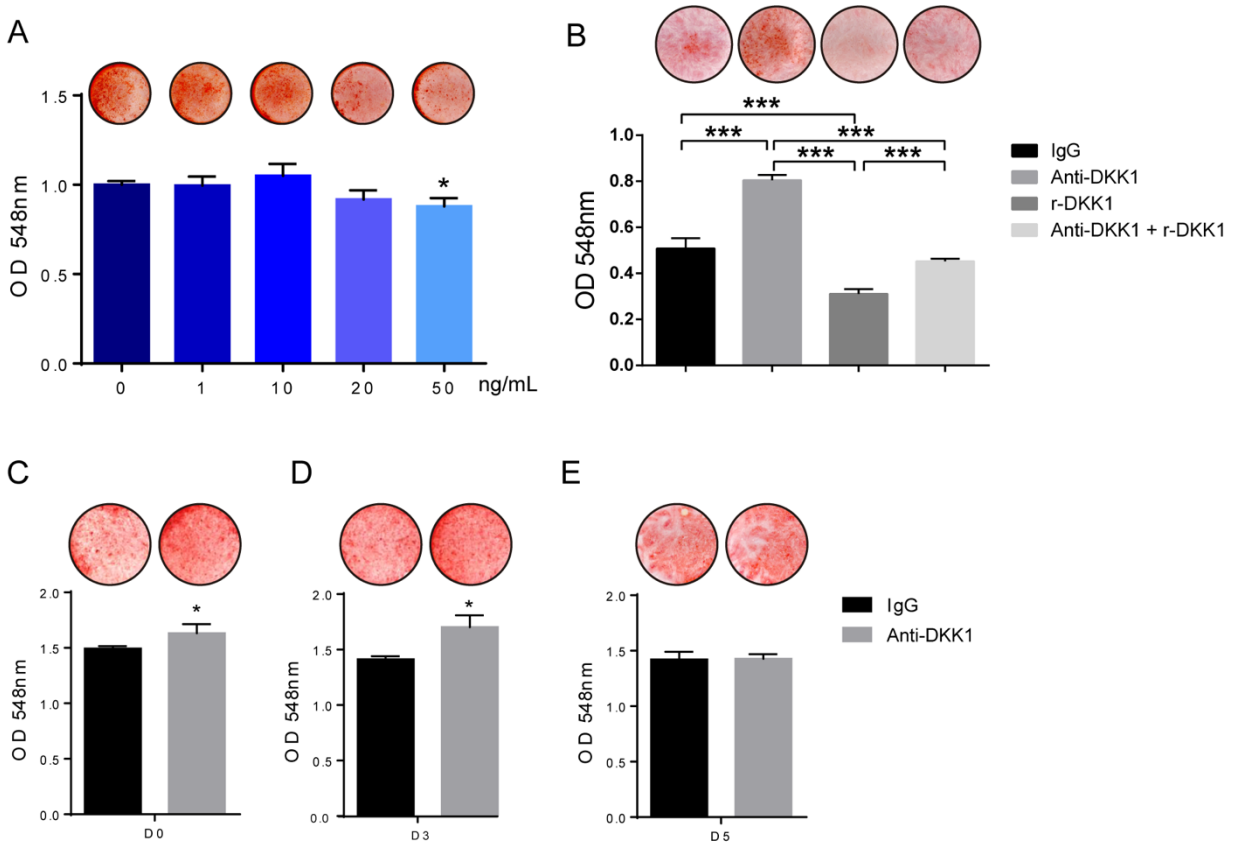

Figure 3. Effects of DKK1 and timing of anti-DKK1 neutralization on ASC osteogenesis. (A) Alizarin red staining (above) and quantification (below) at d 7 of osteogenic differentiation with recombinant DKK1 (1-50 ng/mL). Whole well images shown. **(B)** Alizarin red staining (above) and quantification (below) at d 7 of osteogenic differentiation with DKK1 (50 ng/mL) with or without anti-DKK1 (2 µg/mL). **(C-E)** Effects of anti-DKK1 treatment beginning at different timepoints of osteogenic differentiation. **(C)** Anti-DKK1 treatment (1 µg/mL) initiated at d 0 of osteogenic differentiation, with Alizarin red staining (above) and quantification (below) performed at d 7 of differentiation. **(D)** Anti-DKK1 treatment (1 µg/mL) initiated at d 3, with Alizarin red staining (above) and quantification (below) performed at d 7 of differentiation. **(E)** Anti-DKK1 treatment initiated at d 7 (1 µg/mL), with Alizarin red staining (above) and quantification (below) at d 10 of differentiation. All experiments performed with an appropriate isotype IgG control. Experiments performed in at least experimental and biological triplicate. Error bars represent one standard deviation. **P*<0.05; ****P*<0.001.

- DKK1 antagonism in femoral segmental bone defects

Next, our findings were translated *in vivo* to a critical sized bone defect with or without stem cell treatment. In our experimental study, four groups were compared within a femoral segmental defect model in NOD-*Scid* mice. Treatment groups included: *(1)* acellular scaffold implantation with systemic IgG isotype control treatment or "IgG" (15 mg/kg, SC, twice weekly), *(2)* acellular scaffold implantation with systemic anti-DKK1 treatment or "anti-DKK1" (15 mg/kg, SC, twice weekly), *(3)* human ASC-laden scaffold with systemic IgG isotype treatment or "IgG+ASCs," and *(4)* human ASC-laden scaffold with systemic anti-DKK1 treatment or "Anti-DKK1+ASCs."

Defect sites were surveilled by XR every 4 wks postoperatively (**Fig. 4A**). A qualitative increase in bone growth at the proximal and distal osteotomy sites was appreciated with systemic anti-DKK1 treatment alone or ASC cell therapy in comparison to IgG control. Bone healing was qualitatively most apparent in ASC treatment groups also provided anti-DKK1, in which the bone defect edges approximated one another (far right, **Fig. 4A**). After 8 wks, this qualitative change was confirmed measuring the length of the residual defect span using XR images of each animal (**Fig. 4B**). Combination treatment Anti-DKK1 + ASCs showed a significant reduction in residual defect span, while either cell therapy or anti-DKK1 alone showed a non-significant trend toward reduction in defect span (**Fig. 4B**). The defect site was further analysed using DXA every 4 wks post-operatively (**Fig. 4C**). Here, a gradual increase in BMD was observed across the 8 week time period in all treatment groups. ASC treated defects with anti-DKK1 treatment showed a significant increase in BMD in comparison to other groups (66% increase in comparison to IgG control, 34% increase in comparison to anti-DKK1 alone, and 32% increase in comparison to ASC treated defects with IgG control). In comparison, anti-DKK1 did not increase the BMD at uninjured sites, assessed using both the contralateral femur and lumbar vertebrae (*not shown*), a finding consistent with previously published reports in young mice [35]. In summary, systemic anti-DKK1 improved ASC mediated FSD healing, as shown by increased bone mineral density, and reduced size of the osteoectomy site.

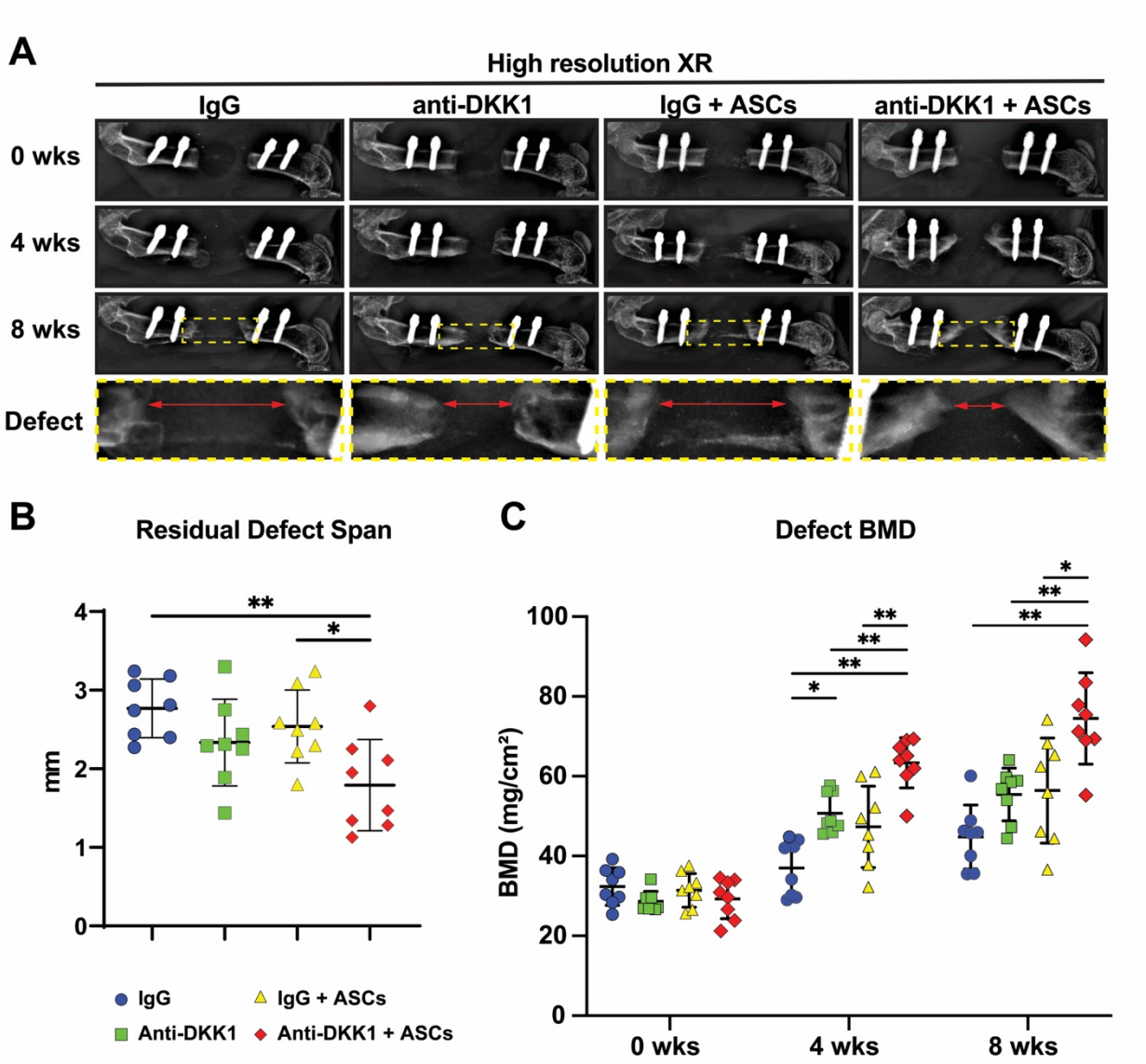

Figure 4. Anti-DKK1 treatment enhances ASC-mediated bone formation in a critical size femoral segmental defect. Defects were treated with ASC seeded scaffolds or acellular control scaffolds. Animals were treated with anti-DKK1 or IgG control (15 mg/kg, sc, twice weekly). (**A**) High resolution roentgenography (XR), immediately postoperatively (0 wks, first row), at 4 wks postoperative (second row), 8 wks postoperative (third row), as well as high magnification of the defect area (bottom row). Each column shows the representative appearance of a treatment group. (**B**) Residual defect span measured on plain films at 8 weeks after surgery. (**C**) Bone mineral density (BMD) of the defect site, as determined by Dual-energy X-ray absorptiometry (DXA) at 0, 4 and 8 wks postoperative. Graphs represent mean and error bars represent one standard deviation. *P<0.05; **P<0.01.

Bone formation within femoral segmental defects was next assessed using high resolution µCT imaging at the study endpoint (**Fig. 5**). Three-dimensional sagittal µCT reconstructions of representative femurs confirmed the impression by XR, again showing an increase in bone formation among ASC treated defects with systemic anti-DKK1 in comparison to other treatment groups **(Fig. 5A-D)**. These radiographic findings were confirmed using quantitative µCT analysis across all animals, including analysis of bone volume (BV), bone volume density (BV/TV), bone mineral density (BMD) **(Fig. 5E-G)**. Here, the combination anti-DKK1 + ASCs treatment group resulted in a significant increase in all metrics in relation to IgG control (22.1-60.7% increase across measured parameters). Trabecular bone analysis showed an increase in trabecular thickness (Tb.Th), although no change in trabecular number (Tb.N) was observed (**Fig. 5H,I**).

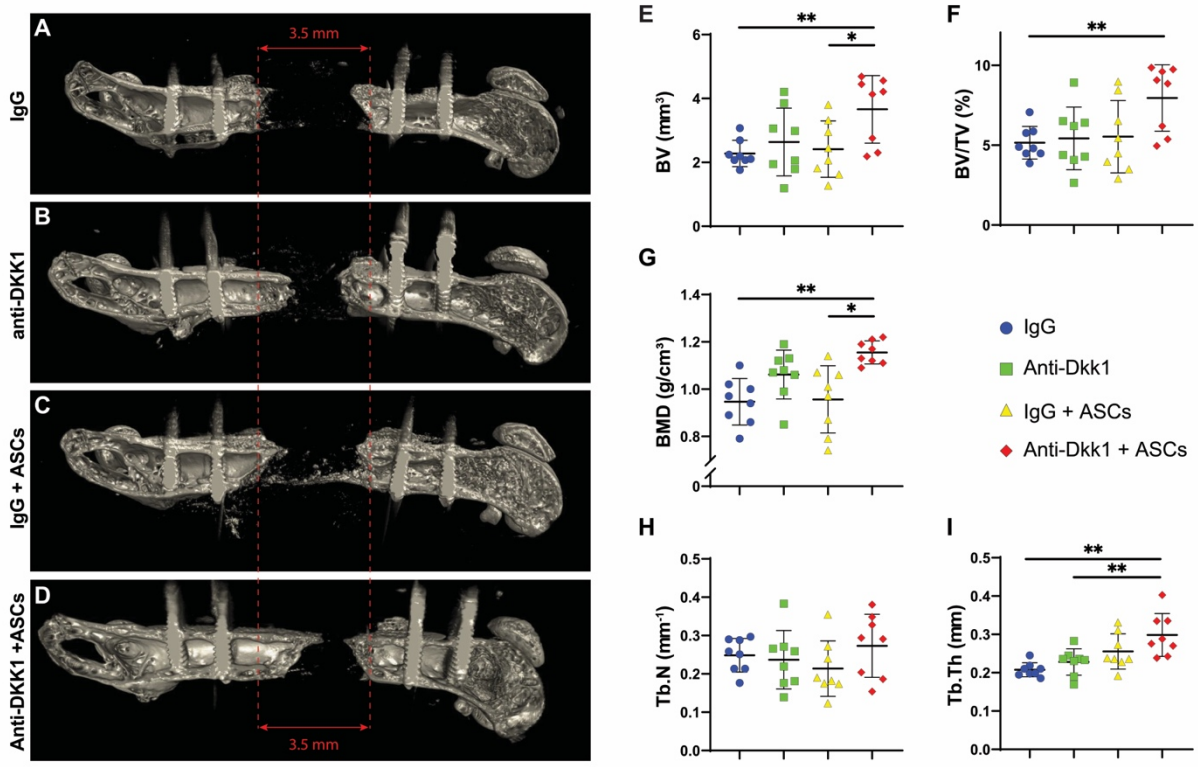

Figure 5. Anti-DKK1 treatment incites ASC-mediated bone formation as assessed by micro computed tomography (µCT). Defects were treated with ASC seeded scaffolds or acellular control scaffolds. Animals were treated with anti-DKK1 or IgG control (15 mg/kg, sc, twice weekly). **(A-D)** Representative three dimensional (3D) µCT reconstructions of the femoral segmental defect (FSD) site at 8 wks post-operative, shown from a sagittal perspective. Original defect size indicated by red lines. **(E-I)** Quantitative µCT analysis of the femoral segmental defect site, including (E) bone volume (BV), (F) fractional bone volume (BV/TV), **(G)** bone mineral density (BMD), **(H)** trabecular number (Tb.N), and **(I)** trabecular thickness (Tb.Th). Dots in scatterplots represent an individual animal, while crosshairs and whiskers represent mean and one SD, respectively. **P*<0.05; ***P*<0.01.

Histological analyses were next performed, which further confirmed morphologic differences associated with systemic anti-DKK1 treatment of ASC treated bone defects (**Fig. 6**). H&E staining among the whole scaffold area (**Fig. 6A-D**) showed bone matrix deposition on the edges of the defect in all the samples, while only the anti-DKK1 + ASCs had robust bone matrix in the middle of the defect (**Fig. 6a'-d'**). Goldner's modified trichrome (GMT) staining confirmed this finding. Within the groups without ASCs therapy, no clear bone matrix deposition was found (**Fig. 6E,F**). Immature bone formation was observed among the IgG + ASCs treatment group (**Fig. 6G**), while prominent woven bone was observed among defect sites among the anti-DKK1 + ASCs group. Safranin O / Fast green (SO/FG) staining was performed, which did not reveal any significant cartilaginous tissue among any treatment group **(Fig. 6I-L).**

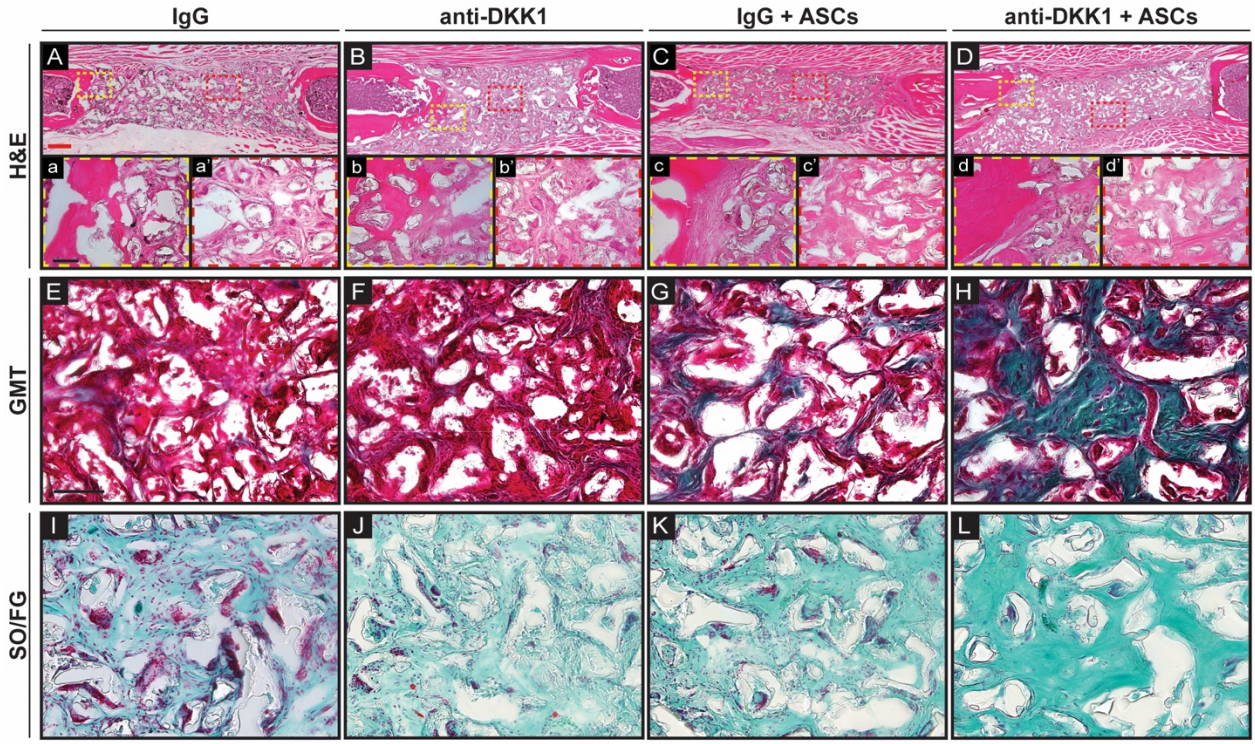

Figure 6. Anti-DKK1 treatment induces ASC-mediated bone matrix formation. Defects were treated with ASC seeded scaffolds or acellular control scaffolds. Animals were treated with anti-DKK1 or IgG control (15 mg/kg, sc, twice weekly). **(A-D)** H&E staining among the entire defect span for each treatment group. High magnification (20x) of (a-d) the bone-scaffold interface and (a'-d') within the implant site. **(E-H)** Goldner's Modified Trichrome (GMT) staining among scaffold area of each group. Bone matrix appears blue/green, while fibrous tissue appears red. **(I-L)** Safranin O/Fast green (SO/FG) staining among scaffold area. Bone matrix appears darker green while cartilage (if present) would appear orange. All analyses performed at 8 weeks post-implantation. Black scale bars: 50 μm; red scale bar: 400 μm.

The osteoblast specific marker osteocalcin (OCN) was next evaluated across the different groups using immunofluorescent staining (**Fig. 7**), cross-reactive with both mouse and human OCN proteins. Images were obtained either at the bone edge / scaffold interface (**Fig. 7A-D**) and within the central aspect of the scaffold areas (**Fig. 7E-H**). A conspicuous increase in OCN immunostaining was present among both ASC cell therapy groups, observable both within the bone-scaffold interface and the central scaffold areas. Across all sections, ASC treated defects with anti-DKK1 administration showed the most conspicuous OCN immunoreactivity.

Osteoclast activity was next assessed using tartrate resistant acid phosphatase (TRAP) stained sections (*not shown*). In general, ASC treated bone defects demonstrated significantly higher TRAP staining than that of acellular controls. ASC treated defects with IgG control treatment showed the most conspicuous TRAP staining across samples. Consistent with known anti-osteoclastic effects of anti-DKK1, the combination treatment anti-DKK1 with ASCs showed a clear reduction in TRAP staining intensity and distribution in comparison to the IgG + ASCs treatment group.

In aggregate, the findings suggest the utility of anti-DKK1 therapies to improve upon stem cell-augmented bone repair. Adipose-derived therapies have potential use for cell-augmented bone repair strategies. Yet, inconsistent repair results in bone tissue engineering have been linked to cell population heterogeneity, variability in cell preparation, or expression of osteogenic differentiation inhibitors. Our observations suggest that DKK1 inhibits the early osteogenic differentiation of human ASCs, and that systemic anti-DKK1 therapy has benefit for the ASC engraftment, survival, and osteodifferentiation, associated with improved defect site revascularization and eventual re-ossification. In this regard, anti-DKK1 is one of only several systemic drugs which has been shown to improve stem cell-augmented bone repair, which also includes intermittent PTH.

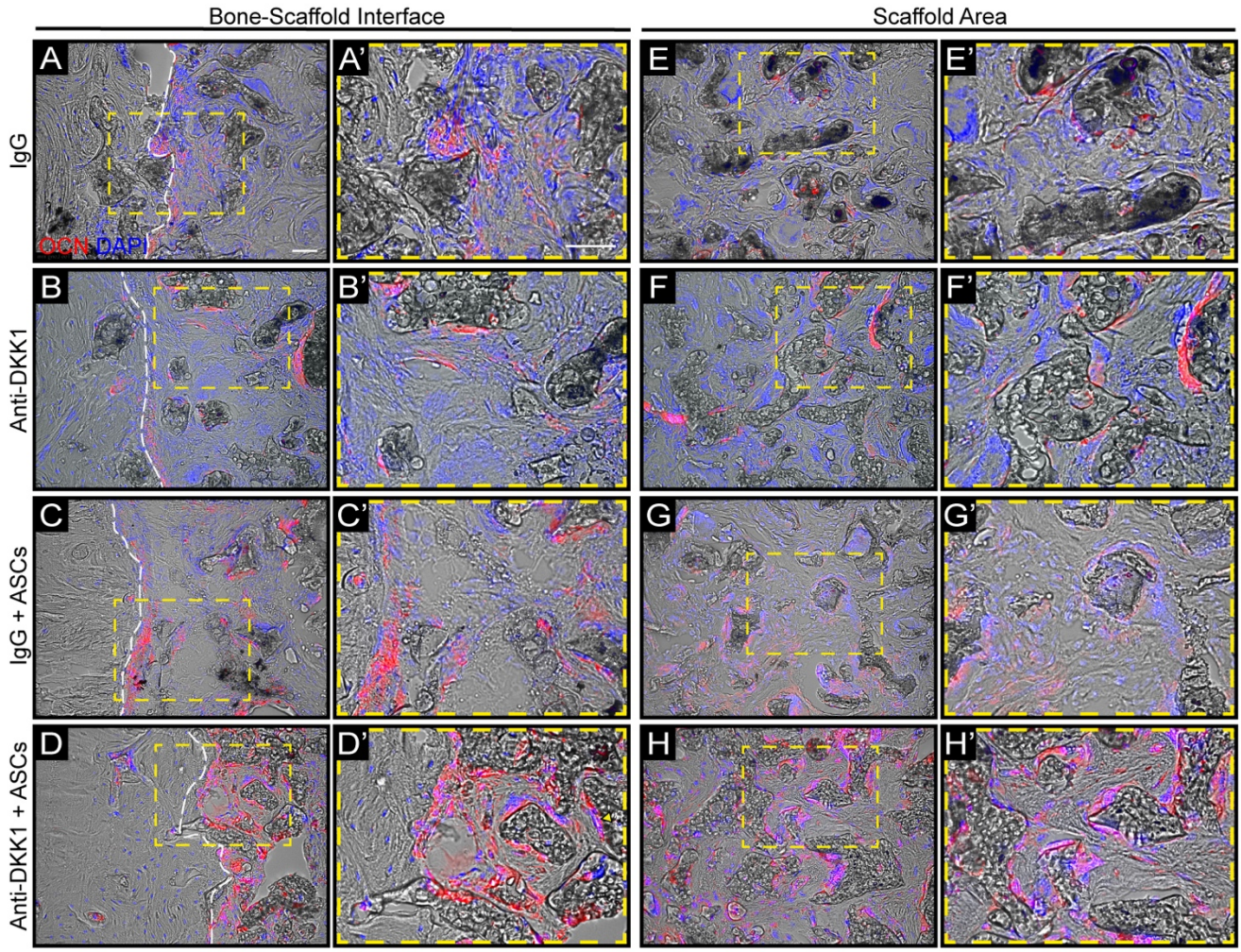

Figure 7. Anti-DKK1 promotes osteoblast differentiation of ASCs and resident osteoprogenitor cells. Defects were treated with ASC seeded scaffolds or acellular control scaffolds. Animals were treated with anti-DKK1 or IgG control (15 mg/kg, sc, twice weekly). Representative osteocalcin (OCN) immunohistochemical staining of the femoral segmental defects, either at the (**A-D**) bone-scaffold interface or (**E-H**) within the implant site. (**A'-H'**) High magnification insets also shown. OCN appears red, while DAPI nuclear counterstain appears blue. White dashed lines outline the bone / scaffold interface. All analyses performed at 8 weeks post-implantation. White Scale bars: 50 μm.

- DKK1 antagonism and spine fusion

Next, we translated our findings in a rat spine fusion model in ovariectomized animals. This represents a significantly more challenging model for bone generation. A small molecule inhibitor of DKK1 was used during the spine fusion process. Female rats underwent ovariectomy (OVX) followed 3 mo later with a spine fusion procedure, with animals treated with or without the DKK1 inhibitor thereafter. First, we corroborated loss of bone mass after OVX surgery showing a significant decreased in lumbar BMD at 5 months (*not shown*). When segregated by treatment groups, there was no significant difference between the treatment and control groups in lumbar BMD. Spines were harvested for analysis 2 mo after the fusion procedure. We observed small molecule drug treatment increases spine fusion rates by microCT imaging and analysis (**Figure 8**). By microCT reconstructions (above) and axial cross-sections (below), increased bone deposition was observed among drug treated animals (**Fig. 8A**). Quantitative analysis by microCT was performed across animals (**Fig. 8B-G**). Results showed a significant increase in Bone Mineral Density (BMD), Bone Volume (BV) and fractional BV (BV/TV) in the spinal fusion site (**Fig. 8B-D**). Trabecular analysis was performed and found a similar trend, including a non-significant increase in trabecular thickness (Tb.Th), significant increase in trabecular number (Tb.N), and a reduction in trabecular spacing (Tb.Sp) (**Fig. 8E-G**).

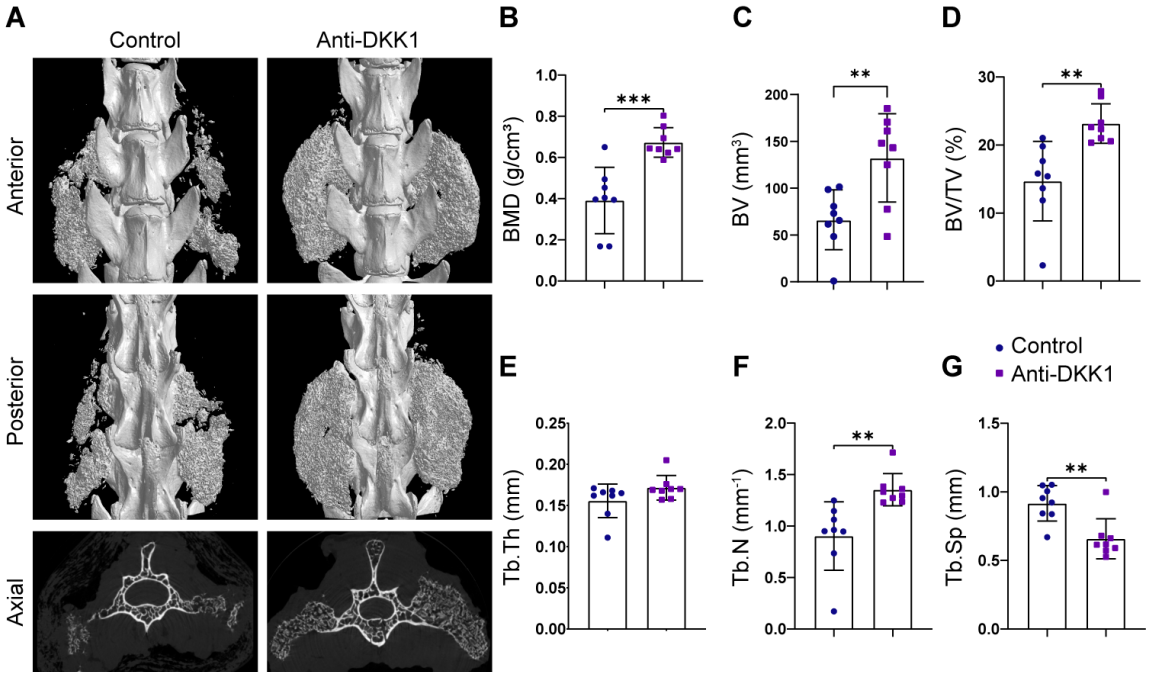

Figure 8: Anti DKK1 drug treatment induces spine fusion in rats. **(A)** MicroCT reconstructions of representative spine fusion segments, including (top) anterior 3D reconstruction, (middle) posterior 3D reconstruction, and (bottom) representative axial cross-section. **(B-G)** MicroCT quantitative analysis, including **(B)** Bone Mineral Density (BMD), **(C)** Bone Volume (BV), **(D)** BV/TV, **(E)** Trabecular Thickness (Tb.Th), **(F)** Trabecular Number (Tb.N), and **(G)** Trabecular Spacing (Tb.Sp). Mean and 1 SD reported, with individual datapoints representing individual animal measurements. **P<0.01; ***P<0.001.

Histologic data demonstrated an increase in bone and cartilage formation at the spine fusion site in small molecule anti-DKK1 treated animals (**Figure 9**). By H&E (**Fig. 9A**) and Goldner's Modified Trichrome staining (**Fig. 9B**), there was a significant increase in bone deposition among treated animals at the spine fusion site. This included a significant increase histologic fusion score (**Fig. 9C**) as well as bone area (**Fig. 9D**). Additional stains were performed including alkaline phosphatase staining and semi-quantitative analysis, which confirmed the same increase in bone formation (**Fig. 9E,F**). Finally Safranin O / Fast Green (SOFG) staining was performed to assess cartilage formation within the spine fusion site. In parallel to bone formation, there was an increase in cartilage area within treated animals (**Fig. 9G,H**).

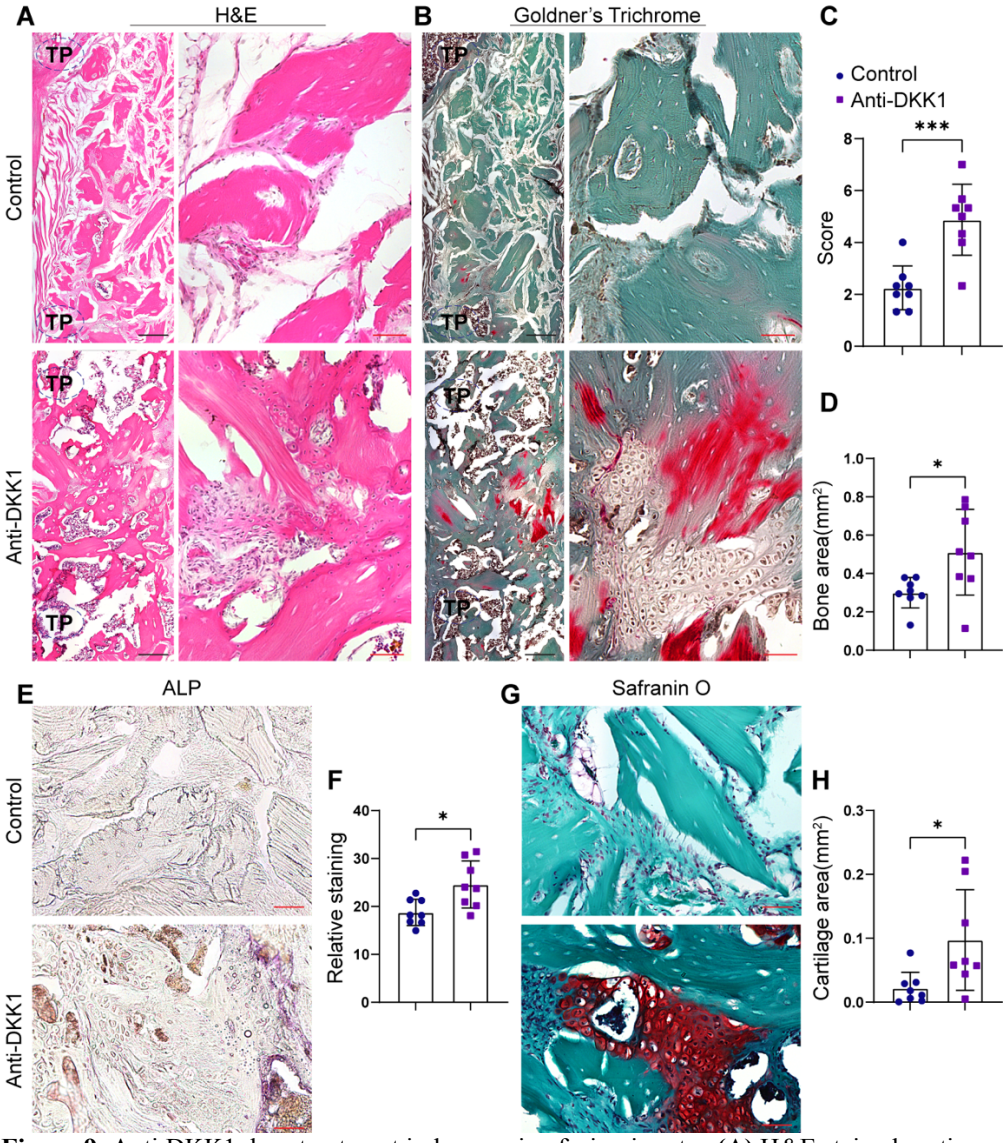

Figure 9: Anti DKK1 drug treatment induces spine fusion in rats. **(A)** H&E stained sections of the spine fusion site (low and high magnification). **(B)** Goldner's modified trichrome stained sections of the spine fusion site (low and high magnification). **(C)** Histologic spine fusion score. **(D)** Bone Area. **(E,F)** Alkaline phosphatase staining and semi-quantification. **(G,H)** Safranin O staining and Cartilage area. (Mean and 1 SD reported, with individual datapoints representing individual animal measurements). *P<0.05; **P<0.01; ***P<0.001.

By immunohistochemical staining, we observed greater accumulation of the osteoblast marker Osteocalcin (OCN) (**Fig. 10A-C**) and the master chondrogenic transcription factor Sox9 (**Fig. 10D,E**). As expected with DKK1 inhibition, we found increased canonical Wnt signaling activity within the bone implantation site, as shown by β-catenin immunofluorescent staining and semi-quantitative analysis (**Fig. 10F,G**). Finally, we examined overall vascularity of the bone implantation site, as some reports suggest that DKK1 regulates vascular ingrowth. Results showed no significant difference in CD31 immunofluorescent staining with or without DKK1 inhibition (**Fig. 10H,I**).

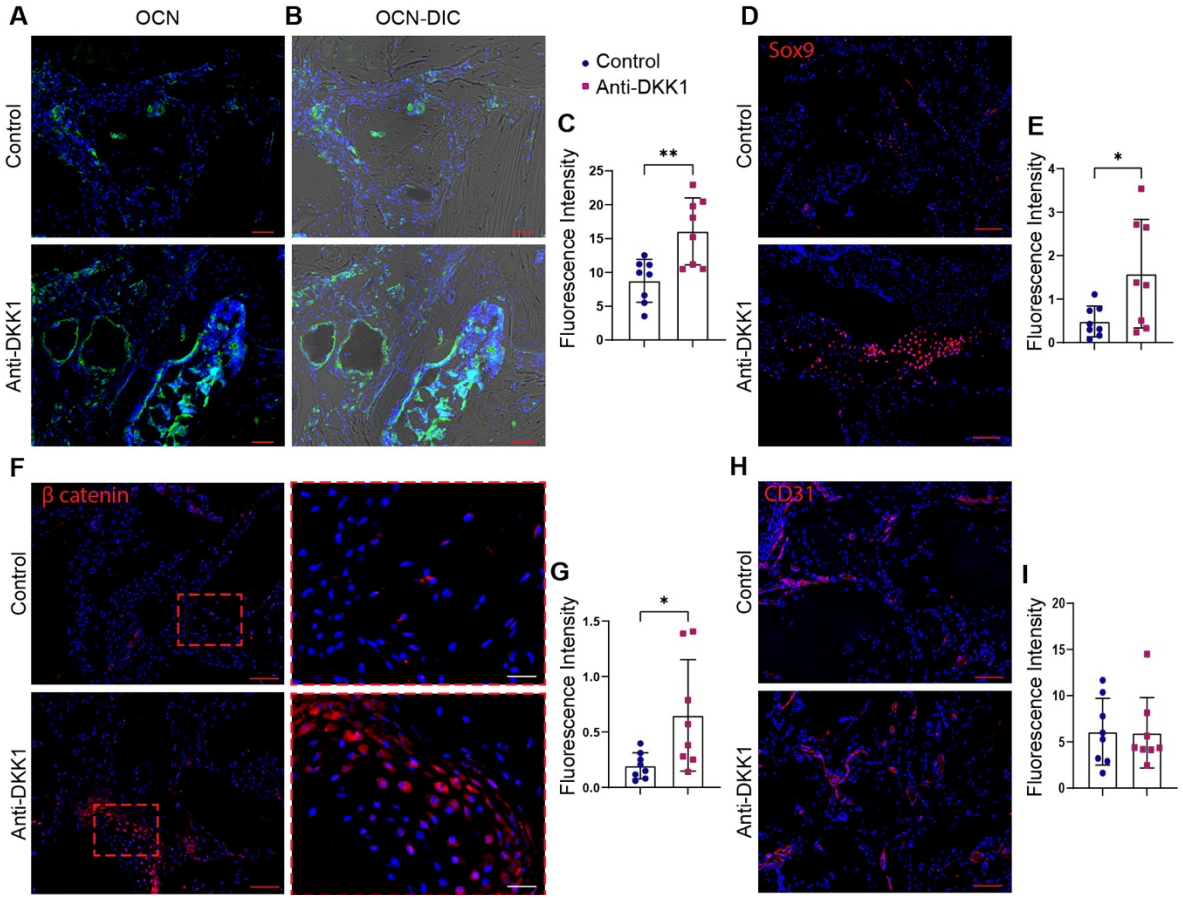

Figure 10. DKK1 inhibition induces bone and cartilage antigen expression during osteoporotic rat spine fusion. All analyses performed 2 mo postoperatively. **(A-C)** Representative images of Osteocalcin (OCN) immunofluorescent staining, shown with or without DIC, and semi-quantitative analysis. **(D,E)** Representative images of Sox9 immunofluorescent staining and semi-quantitative analysis. **(F,G)** Representative images of β-catenin immunofluorescent staining and semi-quantitative analysis. **(H,I)** Representative images of CD31 immunofluorescent staining and semi-quantitative analysis. Red scale bars: 100μm. White scale bars: 25μm. Dots in scatterplots represent an individual animal, while graphs represent mean and error bars represent 1 SD. $*p < 0.05$; $**p < 0.01$.

Key outcomes and conclusions:

Supported by this award, we examined the potential role of anti-DKK1 in bone repair/regeneration and stem cell mediated bone repair. First, we found that anti-DKK1 treatment promoted ASC osteogenic differentiation. As expression levels of DKK1 peaked during early osteogenic differentiation, anti-DKK1 supplemented early but not late during osteogenic differentiation positively regulated osteoblast formation. Furthermore, the capacity of anti-DKK1 to enhance osteogenic differentiation varied between cell batches. Finally, anti-DKK1 led to increased transcript abundance of the Wnt inhibitor *SOST*, potentially representing a compensatory cellular mechanism. These findings were published (Stem Cells Dev, 2020).

Next, we observed that anti-DKK1 treatment can enhance stem cell mediated bone repair in a clinically relevant model of femoral bone injury. Here, systemic anti-DKK1 therapy had benefit for the ASC engraftment, survival, and osteodifferentiation, associated with improved defect site revascularization and eventual re-ossification. In this regard, anti-DKK1 is one of only several systemic drugs which has been shown to improve stem cell-augmented bone repair. These findings were published (Stem Cells Transl Med, 2021).

Finally, we demonstrated that the use of a pharmacological DKK1 inhibitor enhanced posterolateral lumbar fusion in an ovariectomized rat model of osteoporosis. This promotion of bone formation was associated with a clear increase in canonical Wnt/β-catenin signaling. Moreover, we showed an increase in osteoblast activity as well as endochondral ossification. Overall, these observations provide evidence of the potential therapeutic relevance of the use of DKK1 inhibition in the context of bone grafting in healthy or osteoporotic patients. These findings were published (Bone, 2022).

What opportunities for training and professional development has the project provided?

This project provided a number of opportunities for the postdoctoral participants to learn various techniques for stem cell isolation and characterization, stem cell culture and application to orthopaedic animal models, as well as in-depth knowledge of signaling molecules and mechanisms involved in bone regeneration.

How were the results disseminated to communities of interest?

Our novel findings have been disseminated by publication in scientific journals.

What do you plan to do during the next reporting period to accomplish the goals?

N/A

4. IMPACT

What was the impact on the development of the principal discipline(s) of the project?

Overall, we developed and validated anti-DKK1 therapies for the enhancement of stem cell mediated bone repair as well as bone graft mediated spine fusion. This was performed in two clinically relevant orthopaedic models. Overall, we found that systemic anti-DKK1 therapies have several prominent benefits for bone repair / bone generation including improvement of stem cell engraftment and survival, osteogenic and chondrogenic differentiation, improved injury site vascularization and eventual more robust bone formation. In this regard, anti-DKK1 is one of only several systemic drugs which has been shown to improve stem cell-augmented bone repair and/or bone graft mediated bone repair. These findings were published in three separate publications, and are the subject of a current JWMRP grant application under consideration in order to advance our work into large animal models.

What was the impact on other disciplines?

Nothing to Report

What was the impact on technology transfer?

Nothing to Report

What was the impact on society beyond science and technology?

Nothing to Report

5. CHANGES/PROBLEMS

Changes in approach and reasons for change

Nothing to Report

Actual or anticipated problems or delays and actions or plans to resolve them

Nothing to Report

Changes that had a significant impact on expenditures

Nothing to Report

Significant changes in use or care of human subjects, vertebrate animals, biohazards, and/or select agents

Nothing to Report

6. PRODUCTS

- **Publications, conference papers, and presentations**

Journal publications.

1. Wang Y, Negri S, Li Z, Xu J, Hsu CY, Peault B, Broderick K, James AW. Anti-DKK1 enhances the early osteogenic differentiation of human adipose-derived stem/stromal cells. Stem Cells Dev. 2020 Aug 1; 29(15):1007-1015.

2. Negri S, Wang Y, Sono T, Qin Q, Hsu GC, Cherief M, Xu J, Lee S, Tower RJ, Yu V, Piplani A, Meyers CA, Broderick K, Lee M, James AW. Systemic DKK1 neutralization enhances human adipose-derived stem cells mediated bone repair. Stem Cells Transl Med. 2021 Apr;10(4):610-622.

3. Li Z, Xing X, Gomez-Salazar MA, Xu M, Negri S, Xu J, James AW. Pharmacological inhibition of DKK1 promotes spine fusion in an ovariectomized rat model. Bone. 2022 Sep;162:116456.

Books or other non-periodical, one-time publications.

Nothing to Report

Other publications, conference papers and presentations.

Nothing to Report

- ## Website(s) or other Internet site(s)

Nothing to Report

- ## Technologies or techniques

Nothing to Report

- ## Inventions, patent applications, and/or licenses

Nothing to Report

- ## Other Products

Nothing to Report

7. PARTICIPANTS & OTHER COLLABORATING ORGANIZATIONS

What individuals have worked on the project?

Name:	Aaron James
Project Role:	PI
Researcher Identifier	https://orcid.org/0000-0002-2002-622X
Nearest person month worked:	1.1
Contribution to Project:	Dr. James has overseen all aspects of the project.
Funding Support:	NIH, DoD, American Cancer Society, Maryland Stem Cell Research Fund, ALSF

Name:	Chia Soo, MD
Project Role:	Co-I
Researcher Identifier	None
Nearest person month worked:	0.6
Contribution to Project:	Dr. Soo has consulted with Dr. James regarding the surgical approach aim 2 and 3 studies, providing surgical expertise.

Funding Support:	NIH

Name:	Bruno Peault, PhD
Project Role:	Co-I
Researcher Identifier	None
Nearest person month worked:	0.6
Contribution to Project:	Dr. Peault has compared the pro-osteogenic effects of anti-DKK1 on purified PSC in vitro
Funding Support:	NIH

Name:	Mary Archer
Project Role:	Lab Manager
Researcher Identifier	
Nearest person month worked:	0.4
Contribution to Project:	Mrs. Archer assists in overseeing all aspects of the project.
Funding Support:	NIH, DoD, American Cancer Society

Name:	Masnsen Cherief, PhD
Project Role:	Postdoctoral Researcher
Researcher Identifier	
Nearest person month worked:	8.4
Contribution to Project:	Dr. Cherief assisted in the radiographic and histologic analysis of in vivo studies, in conjunction with Dr. James.
Funding Support:	NIH, PNNR

Name:	Seungyong Lee
Project Role:	Postdoctoral Researcher
Researcher Identifier	
Nearest person month worked:	2.3
Contribution to Project:	Dr. Lee performs the majority of in vitro and in vivo experimental procedures in conjunction with Dr. James.
Funding Support:	NIH, DoD,

Name:	Qizhi Qin
Project Role:	Postdoctoral Researcher
Researcher Identifier	
Nearest person month worked:	2.0
Contribution to Project:	Dr. Qin assisted in the radiographic and histologic analysis of in vivo studies.
Funding Support:	NIH, DoD

Name:	Mario Gomez - Salazar, PhD
Project Role:	Postdoctoral Researcher
Researcher Identifier	
Nearest person month worked:	1.2
Contribution to Project:	Dr. Gomez-Salazar assisted in the radiographic and histologic analysis of in vivo studies.
Funding Support:	NIH, DoD

Has there been a change in the active other support of the PD/PI(s) or senior/key personnel since the last reporting period?

Nothing to Report

What other organizations were involved as partners?

University of California, Los Angeles
10920 Wilshire Blvd., Ste. 600
Los Angeles, CA 90024

8. SPECIAL REPORTING REQUIREMENTS

COLLABORATIVE AWARDS:

Not applicable

QUAD CHARTS:

Dkk1 Antagonism for Stromal Vascular Fraction (SVF) Mediated Bone Repair

BA160256
W81XWH-18-10613

PI: Aaron W. James, MD, PhD **Org:** Johns Hopkins University / UCLA **Award Amount:** 1,364,077

Study/Product Aim(s)

- Determine how DKK1 antagonism impacts human ASC lineage commitment in vitro (Aim 1)
- Validate the combination of anti-DKK1 and SVF in femoral bone defect regeneration (Aim 2)
- Challenge anti-DKK1 and SVF therapy in osteoporotic lumbar spine fusion (Aim 3)

Approach

Non-healing bone defects remain a significant problem for combat casualties and military veterans. Mesenchymal stem cells (MSC) accelerate bone regeneration, yet current MSC treatments have cell heterogeneity with variable and decreased bone-forming efficacy. Our past studies have led us to the primary hypotheses that *(1)* DKK1 may represent a targetable 'molecular brake' on the osteogenic differentiation of human SVF, and *(2)* that 'release' of this brake via use of neutralizing anti-DKK1 antibody treatment may 'rescue' the poor bone-forming efficacy of SVF. Here, we examine this in a combined in vitro / in vivo approach in human cells, as well as mouse and rat models of bone repair.

Timeline and Cost

Activities / CY	18	19	20	21	22
In vitro studies (Major task 1)					
Mouse studies (Major task 2)					
Rat studies (Major task 3)					
Estimated Budget ($K)	**$230**	**$286**	**$278**	**$283**	**$286**

Updated: (01/20/2023)

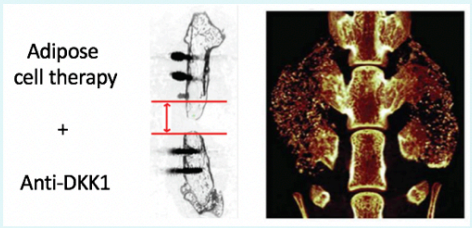

The proposed work combines human adipose-derived cellular therapies with anti-DKK1 for improved bone regeneration, either in a mouse femoral segmental defect model (middle) or rat lumbar spine fusion model (right).

Accomplishment: We have demonstrated the potential for anti-DKK1 and DKK1 inhibition therapies for bone repair / bone formation, and cell-augmented bone repair / bone generation in mouse and rat models..

Goals/Milestones

CY18 Goal – Evaluate anti-DKK1 in vitro
☑ Evaluated osteogenic effects of anti-DKK1 in vitro
CY19 Goals – Initiate in vivo mouse anti-DKK1 studies
☑ Perform initial surgical studies in mice
CY20 Goals – Complete mouse studies, initiate rat anti-DKK1 studies
☑ Perform histologic analyses of anti-DKK1 studies in mice
☑ Initiate rat spine fusion studies
CY21-22 Goals – Continue rat spine fusion anti-DKK1 studies
☑ Complete rat spine fusion anti-DKK1 studies

Comments/Challenges/Issues/Concerns

- None.

Budget Expenditure to Date
Projected Expenditure: $1,364,077
Actual Expenditure: $1,364,077

9. APPENDICES:

Not applicable